Electronic Supplementary Information

Ultra-large electromechanical deformation in lead-free piezoceramics at reduced thickness

Xiang He,[abc] Muzaffar Ahmad Boda,[a] Chen Chen,[a] Rongmin Dun,[abc] Lu Wang,[ab] Yizheng Bao,[a] Dongfang Pang,[d] Lin Guo,[c] Huarong Zeng,[ab] Yongxiang Li[e] and Zhiguo Yi*[abc]

[a] State Key Laboratory of High Performance Ceramics and Superfine Microstructure, Shanghai Institute of Ceramics, Chinese Academy of Sciences, Shanghai 200050, China.

[b] Center of Materials Science and Optoelectronics Engineering, University of Chinese Academy of Sciences, Beijing 100049, China.

[c] CAS Key Laboratory of Optoelectronic Materials Chemistry and Physics, Fujian Institute of Research on the Structure of Matter, Chinese Academy of Sciences, Fuzhou 350002, China.

[d] College of Rare Earths, Jiangxi University of Science and Technology, Ganzhou 341000, China.

[e] School of Engineering, RMIT University, Melbourne VIC 3000, Australia.

*E-mail: zhiguo@mail.sic.ac.cn; zhiguo@fjirsm.ac.cn

This PDF file includes:

Experimental section

Figs. S1 to S15

Other Supplementary Materials for this manuscript include the following:

Videos S1 to S4

Experimental section

Preparation of BNT-BT, BNT, CBNO, KNN, BCZT, BS-PT and $SrTiO_3$ ceramics

All ceramic powders in this work were fabricated by conventional solid-state reaction method. High-purity Bi_2O_3 (99.99%), Na_2CO_3 (99.8%), K_2CO_3 (99.99%), $BaCO_3$ (99.0%), TiO_2 (99.99%), $CaCO_3$ (99.95%), Nb_2O_5 (99.9%), Sc_2O_3 (99.9%), PbO (99.9%), $SrTiO_3$ (99.5%) and $BaZrO_3$ (99.0%) powders were mixed according to the corresponding stoichiometry by ball milling for 10 h. Next, these mixtures for BNT-BT, BNT and CBNO were prepared by double calcination at 850 and 880°C for 2 h. KNN powder was prepared by double calcination at 730 and 930 °C for 4 h. BCZT powder was prepared by calcination at 1250 °C for 6 h. BS-PT powder was prepared by double calcination at 800 and 850 °C for 4 h. After re-milling and collecting, the calcined BNT-BT, BNT, BCZT and CBNO powders were mixed with 5wt% polyvinyl alcohol (PVA) and pressed into compacted disks of 10 mm in diameter and 1 mm in thickness. After burning off the PVA at 600 °C for 4 h, the BNT-BT, BNT, BCZT and CBNO green pellets embedded in their mother powder were sintered at 1150 °C for 2 h, 1140 °C for 2 h, 1450 °C for 6 h and 1150 °C for 3 h, respectively, in sealed alumina crucibles. The KNN, BS-PT and $SrTiO_3$ ceramics were sintered by a spark plasma sintering furnace (Model SPS-211LX, Fuji Electronic Industrial CO., Ltd, Japan) in a 10 mm diameter graphite die under 40 MPa at 980 °C for 4 min, 950 °C for 2 min and 1250 °C for 2 min, respectively. The SPS sintered KNN, BS-PT and $SrTiO_3$ ceramics were further polished to ~0.35 mm thickness and then annealed in a high-purity oxygen atmosphere at 880 °C for 4 h, 850 °C for 4 h and 1400 °C for 6 h, respectively.

Structure characterization and performance measurements

The surface phase structures of all ceramics were identified by using desktop XRD equipped with Cu Kα radiation (Miniflex600, Rigaku, Japan). The microstructures were observed using field emission scanning electron microscope (SEM, SU-8010, Hitachi, Japan) and transmission electron microscopy (TEM, JEM-2100F, JEOL, Japan). The surface chemical states were analyzed by X-ray photoelectron spectroscopy (Thermo Scientific K-Alpha, America). All of the XPS peaks were calibrated using the

adventitious carbon signal (C 1*s*) at 284.8eV. All samples were thinned to desired thickness by lapping with 1500-grit SiC paper and further mirror-polishing with 50 nm diamond suspension, and then pasted with silver electrodes on both surfaces for electric tests. The dielectric permittivity/loss-temperature curves were measured by an LCR meter (TH2828S, Changzhou, China) at a heating rate of 2 °C/min. The ferroelectric and corresponding displacement measurements were carried out by a ferroelectric test system (TF Analyzer 2000E; aixACCT, Aachen, Germany). The sinusoidal alternating electric field applied to deformable mirror device was generated by a signal generator (33120A, Agilent, America) and a voltage amplifier (PZD2000A, Trek, America).

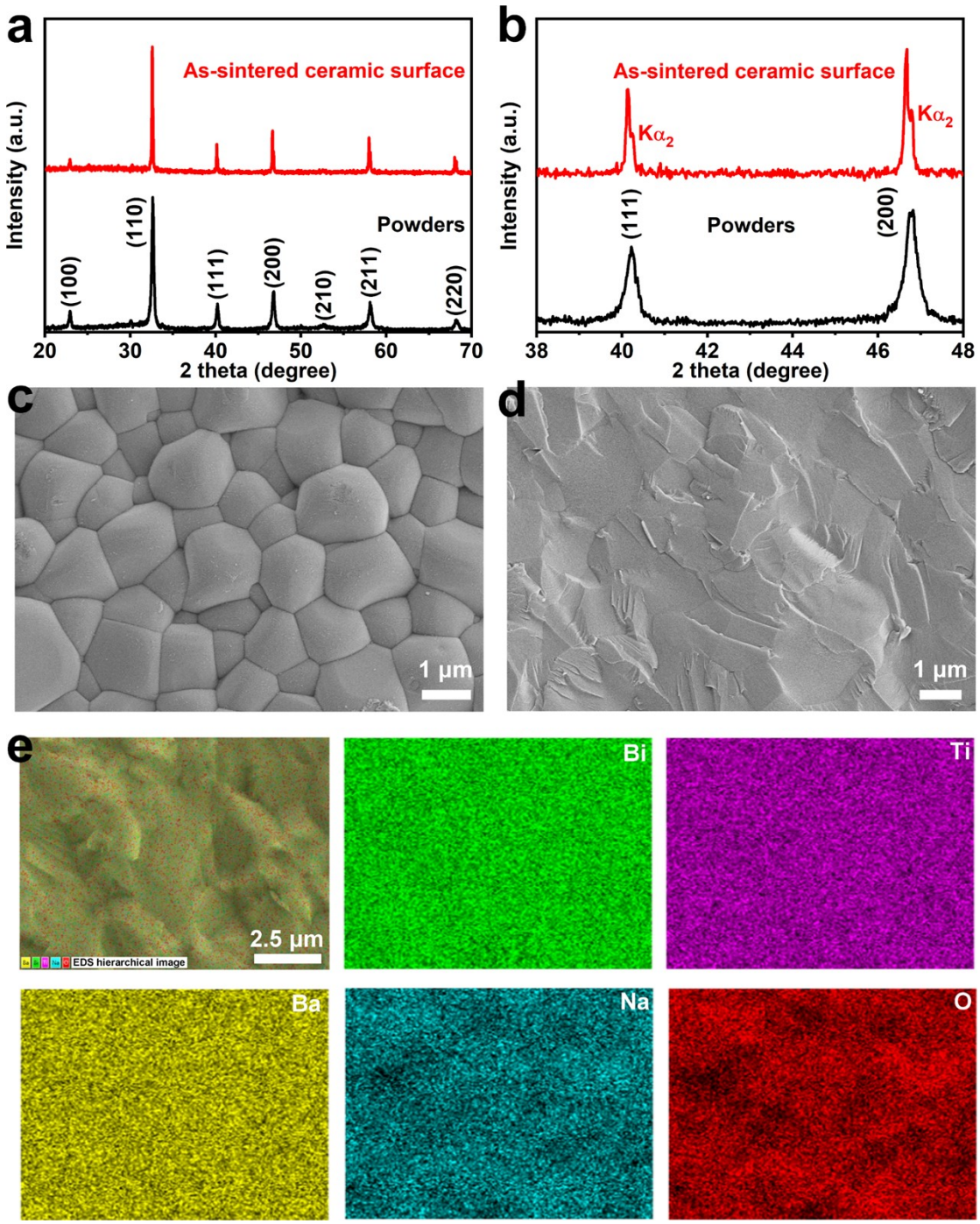

Fig. S1 Structure characterization of BNT-BT ceramics. (**a**) XRD patterns of BNT-BT ceramic plates and crushed powders. (**b**) The enlarged XRD profiles in the 2 theta range of 38° to 48°. (**c,d**) SEM images of the ceramic surface (**c**) and fracture surface (**d**). (**e**) The fracture surface energy-dispersive spectrum (EDS) hierarchical image and corresponding element mapping of Bi, Ti, Ba, Na and O, respectively.

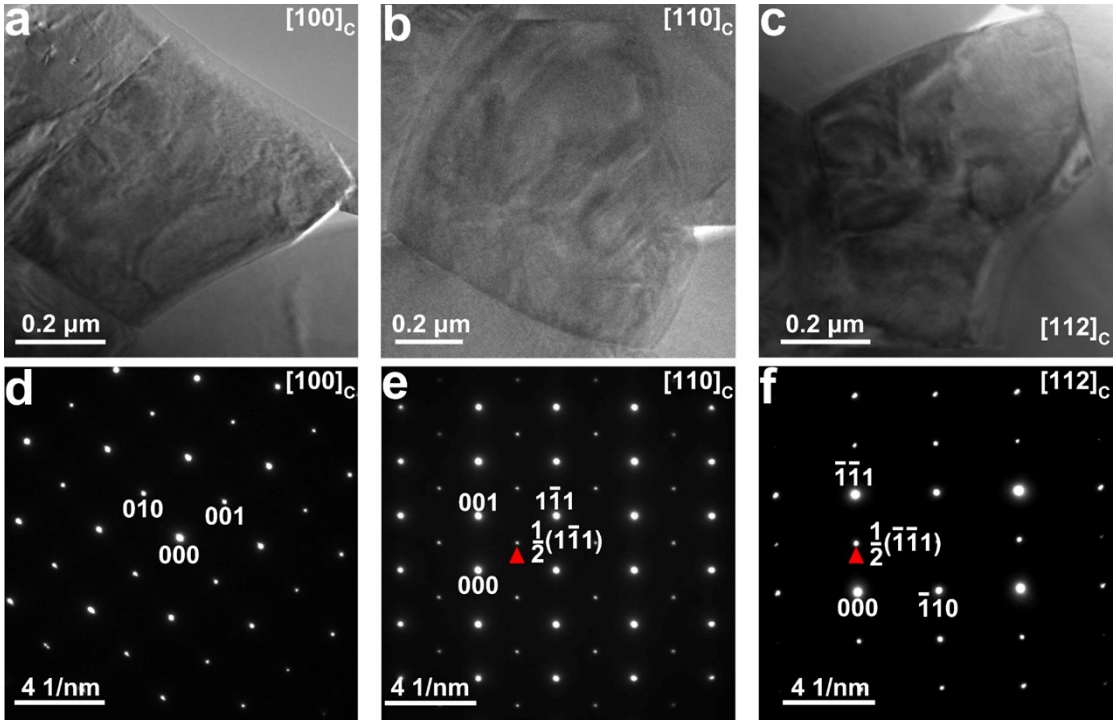

Fig. S2 Transmission electron microscopy images of BNT-BT ceramics. (**a-c**) Bright-field TEM images of the domain structures; (**d-f**) Selected area electron diffraction patterns recorded along $[100]_C$, $[110]_C$ and $[112]_C$ zone axes, respectively. As a typical relaxor ferroelectric, all three grains exhibit irregular nanodomain morphologies and the diffraction characteristics of single rhombohedral (R) phase. These results (Fig. S1 and S2) suggest that BNT-BT ceramics possess the component homogeneity from macro to micro dimensions.

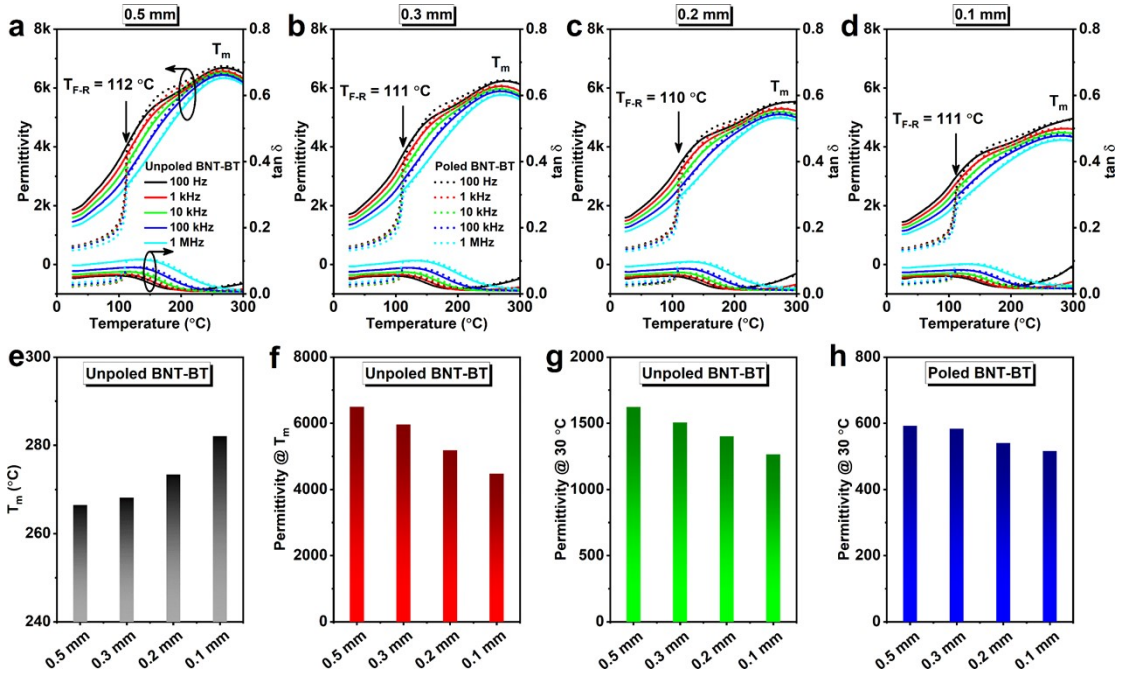

Fig. S3 Dielectric performance of BNT-BT ceramics with various thickness. (**a-d**) Temperature dependence of permittivity of BNT-BT ceramics with thickness of 0.5 mm (**a**), 0.3 mm (**b**), 0.2 mm (**c**) and 0.1 mm (**d**). T_{F-R}: ferroelectric-relaxor transition temperature. T_m: temperature with the maximum dielectric permittivity. (**e-h**) Values of T_m (**e**), maximum dielectric permittivity (**f**), room temperature dielectric permittivity of unpoled ceramics (**g**) and room temperature dielectric permittivity of poled ceramics (**h**) as a function of thickness.

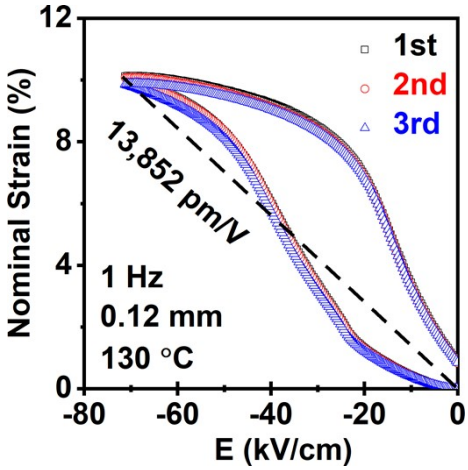

Fig. S4 The unipolar *S*-*E* curves of thin BNT-BT ceramics (0.12 mm in thickness) under negative electric field at 130 °C.

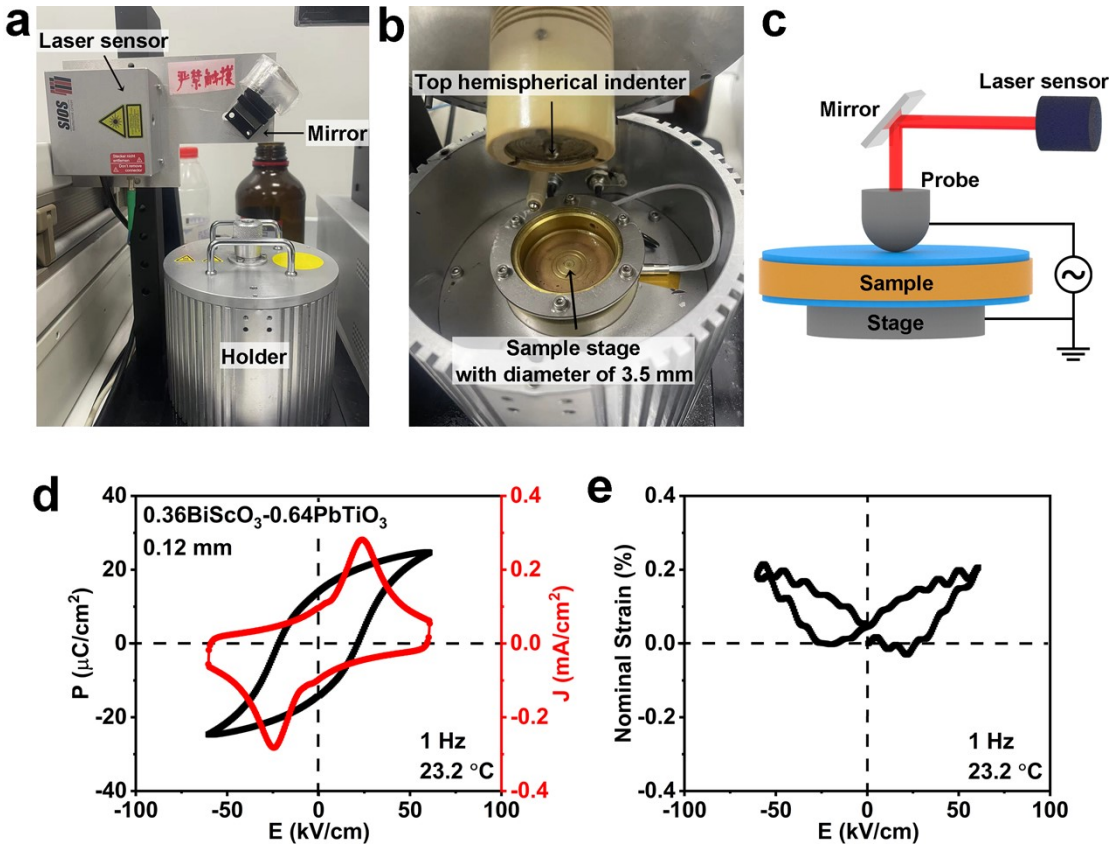

Fig. S5 Commercial strain test system equipped with a laser interferometer. (**a**) Photograph of the sample holder and laser displacement sensor for bulk ceramic samples. (**b**) Photo inside the holder. (**c**) Corresponding schematic illustration of the strain test system. (**d,e**) The polarization-electric field (*P*-*E*) hysteresis loops, current density-electric field (*J*-*E*) curves and bipolar electric field-induced strain (*S*-*E*) curves of a $0.36BiScO_3$-$0.64PbTiO_3$ ceramic (0.12 mm in thickness and 8.0 mm in diameter), measured using this test system at room temperature and 1 Hz.

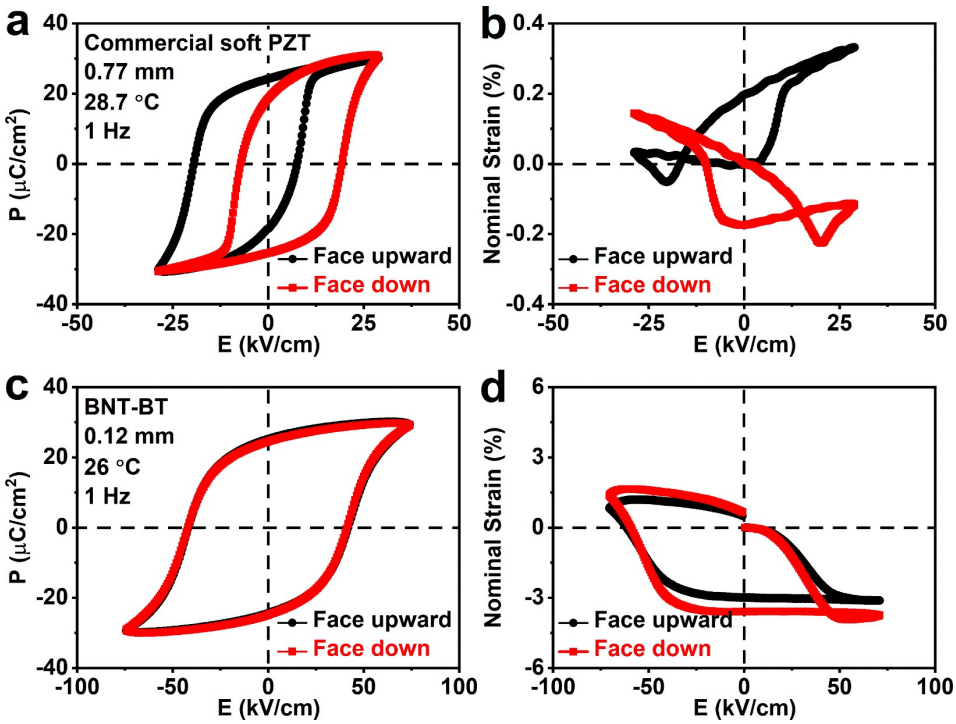

Fig. S6 Modulating the *S*-*E* curves by flipping the testing sample. (**a,c**) The bipolar *P*-*E* and (**b,d**) *S*-*E* curves of commercial soft PZT ceramics (0.77 mm in thickness, **a,b**) and thin BNT-BT ceramics (0.12 mm in thickness, **c,d**) with facing upward and down. It should be noted that the soft PZT ceramics were poled under 40 kV/cm for 15 min and then aged at room temperature for more than 1 year.

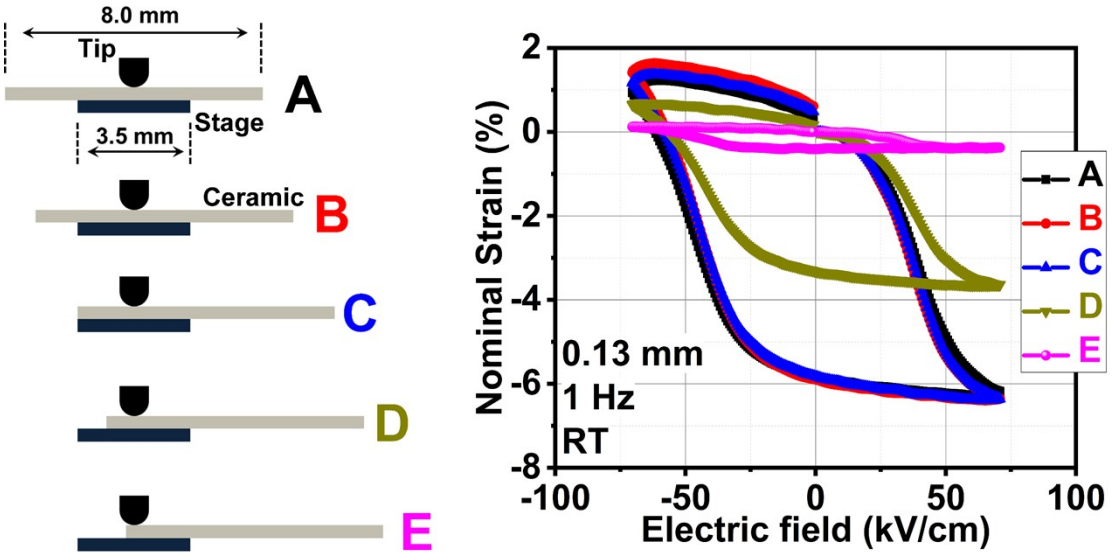

Fig. S7 The position dependence of the *S*-*E* curves. A, B, C, D and E represent the different positions of BNT-BT ceramic sample (8.0 mm × 4.0 mm × 0.13 mm) on the sample stage.

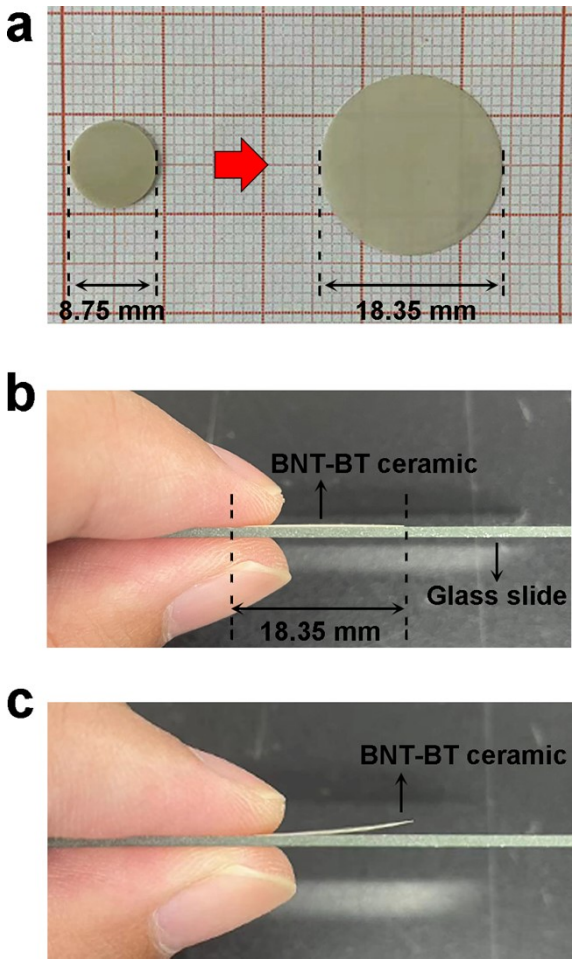

Fig. S8 Macroscopic bending deformation in BNT-BT ceramics. (**a**) Photograph of BNT-BT ceramics with diameters of 8.75 mm and 18.35 mm, respectively. (**b,c**) Photos of a large thin BNT-BT ceramic plate (0.12 mm in thickness and 18.35 mm in diameter) before ferroelectric measurement (**b**) and after applying a positive voltage on the top surface (**c**).

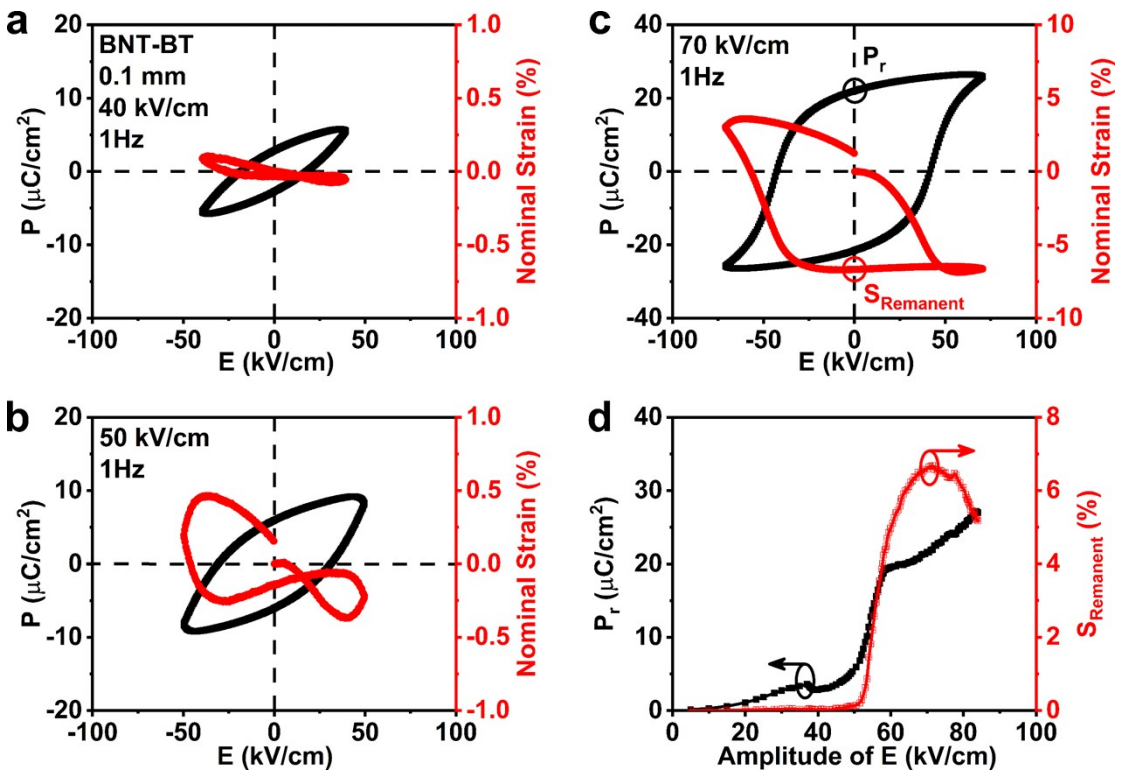

Fig. S9 Polar behavior of thin BNT-BT ceramics at different electric fields. (**a-c**) The *P-E* and nominal *S-E* curves of BNT-BT ceramics (0.1 mm in thickness) at 40 kV/cm (**a**), 50 kV/cm (**b**) and 70 kV/cm (**c**). (**d**) Electric field dependence of P_r and $S_{Remanent}$ of BNT-BT ceramics with thickness of 0.1 mm.

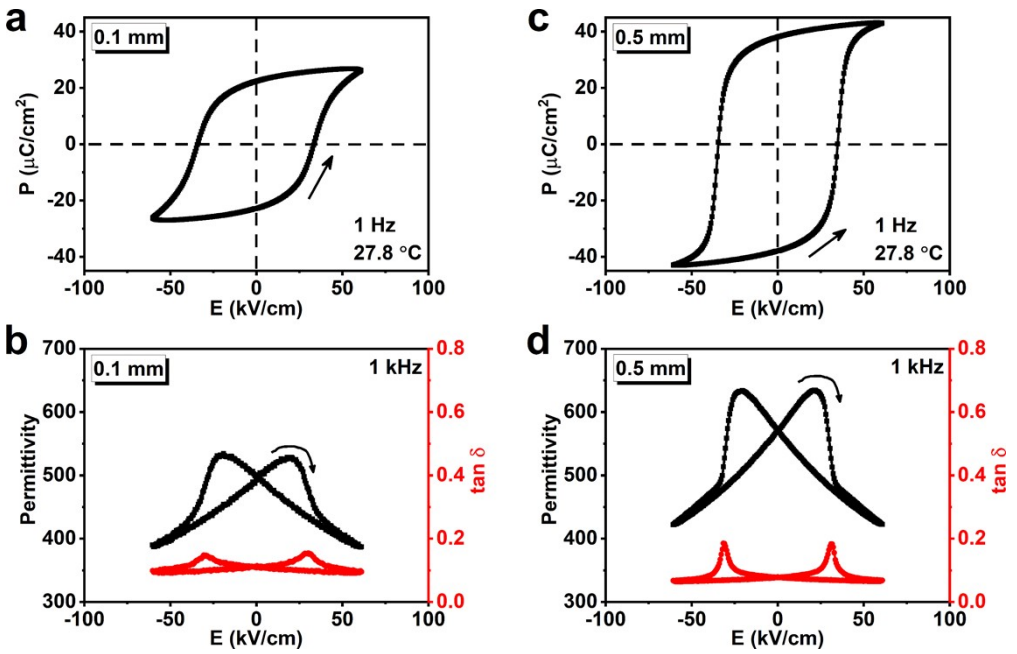

Fig. S10 (**a**,**c**) Polarization-electric field curves and (**b**,**d**) electric field dependent dielectric permittivity of BNT-BT ceramics with thickness of 0.1 mm (**a**,**b**) and 0.5 mm (**c**,**d**). Dielectric permittivity-electric field (ε_r-E) curves were carried out in a Ferroelectric tester (TF Analyzer 2000E; aixACCT, Aachen, Germany), by superimposing a small AC signal ($V_{p\text{-}p}$ = 12 V @ 1 kHz for thin ceramics, $V_{p\text{-}p}$ = 60 V @ 1 kHz for thick ceramics) on a DC bias voltage sweeping quasi-statically from zero to positive and then to negative.

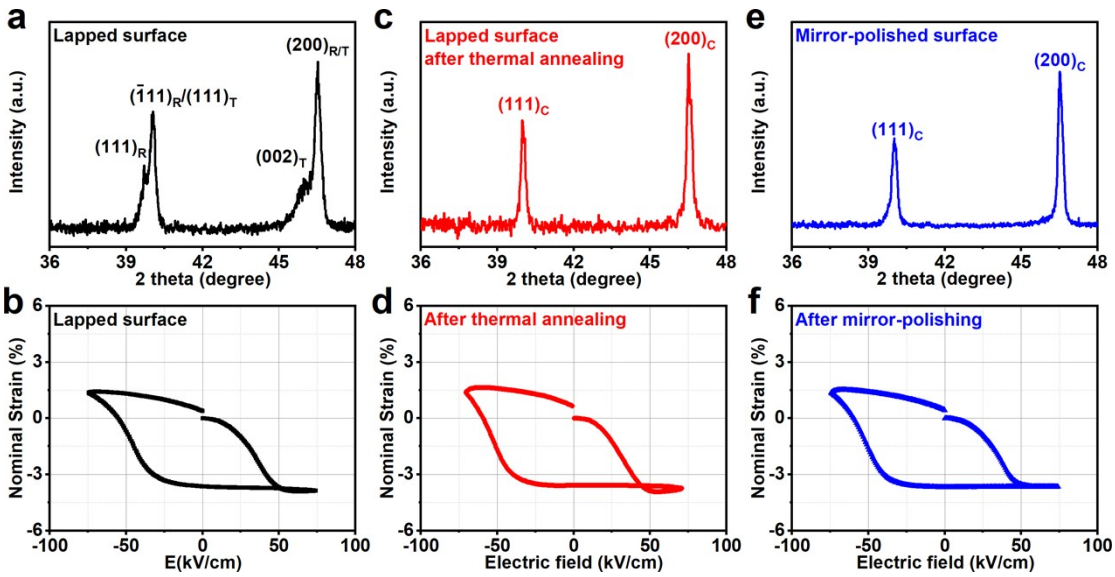

Fig. S11 Surface phase analyses and *S*-*E* curves of thin BNT-BT ceramics with various surface treatments. (**a,c,e**) XRD patterns and (**b,d,f**) bipolar nominal *S*-*E* curves of thin BNT-BT ceramics (0.12 mm in thickness) with lapped surface (**a,b**), after post-annealing at 800 °C for 4 hours (**c,d**) and after mirror-polishing (**e,f**).

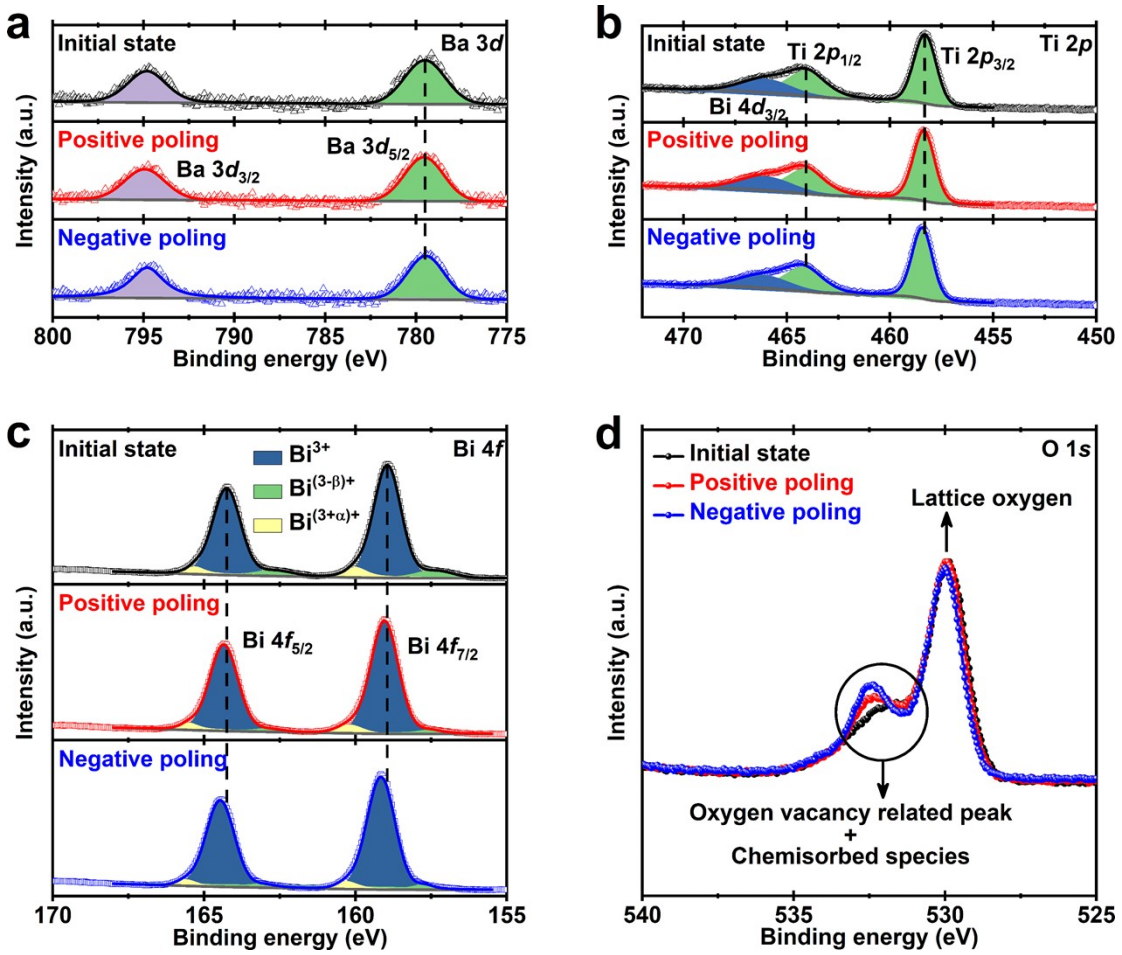

Fig. S12 Surface chemical state of BNT-BT samples. The high-resolution XPS spectra of the (**a**) Ba 3*d*, (**b**) Ti 2*p*, (**c**) Bi 4*f* and (**d**) O 1*s* of a BNT-BT ceramic surface after different poling treatment. The Bi $4f_{5/2}$ and Bi $4f_{7/2}$ spectra were carefully fitted by three separated peaks, representing a mixture of Bi^{3+}, lower valence $Bi^{(3-\beta)+}$ and higher valence $Bi^{(3+\alpha)+}$.

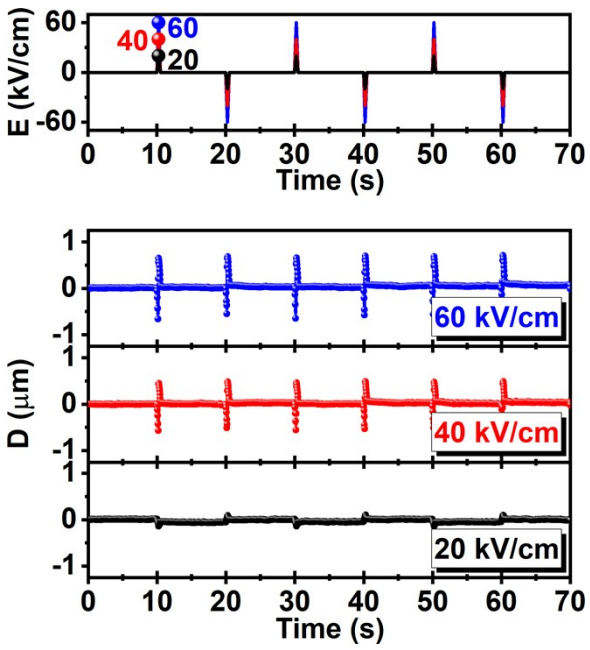

Fig. S13 Pulsed electric field driven probe displacement response at various magnitudes of electric field for a BNT-BT ceramics with thickness of 0.5 mm.

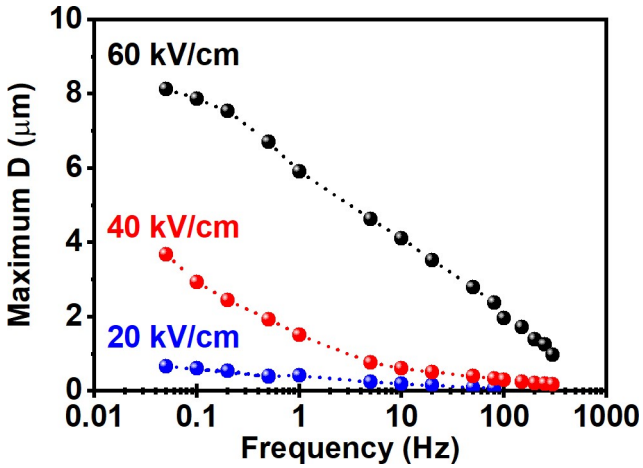

Fig. S14 Frequency-dependent maximum displacement of the capacitor-like actuator made of BNT-BT with thickness of 0.12 mm. Evolution of maximum displacement output as a function of driving frequencies ($0.05 \leq f \leq 300$ Hz), excited by different electric fields with amplitudes of 60, 40 and 20 kV/cm for 10 cycles.

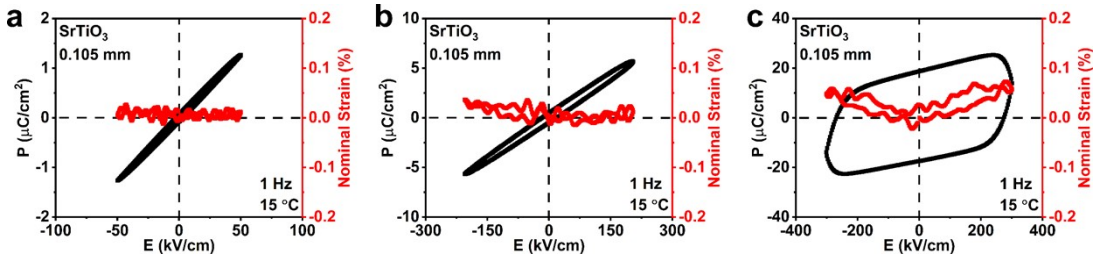

Fig. S15 The effect of thickness on the symmetry of the strain curves in non-ferroelectric ceramics. The bipolar *P*-*E* and *S*-*E* curves of a non-ferroelectric ceramic $SrTiO_3$ (0.105 mm in thickness) at (**a**) 50 kV/cm, (**b**) 200 kV/cm and (**c**) 300 kV/cm.

Video S1 Real-time video showing the bending deformation of a BNT-BT cantilever (4.3 mm × 0.125 mm × 23 mm) driven by a triangular-waveform a.c. voltage (600 V and 1 Hz).

Video S2 When a negative voltage (-750V) is applied to the upper surface, the BNT-BT cantilever (4.3 mm × 0.125 mm × 23 mm) will curve downwards.

Video S3 When a positive voltage (750 V) is applied to the upper surface, the BNT-BT cantilever (4.3 mm × 0.125 mm × 23 mm) will curve upwards.

Video S4 Ultra-high tip displacement output of a BNT-BT cantilever (4.3 mm × 0.125 mm × 23 mm) excited by a sinusoidal electric field of 22.4 kV/cm at resonant frequency point.